Colorectal Cancer Classification using Deep Convolutional Networks
An Experimental Study

Francesco Ponzio, Enrico Macii, Elisa Ficarra and Santa Di Cataldo

Department of Control and Computer Engineering, Politecnico di Torino, Corso Duca degli Abruzzi 24, 10129 Torino, Italy

Abstract: The analysis of histological samples is of paramount importance for the early diagnosis of colorectal cancer (CRC). The traditional visual assessment is time-consuming and highly unreliable because of the subjectivity of the evaluation. On the other hand, automated analysis is extremely challenging due to the variability of the architectural and colouring characteristics of the histological images. In this work, we propose a deep learning technique based on Convolutional Neural Networks (CNNs) to differentiate adenocarcinomas from healthy tissues and benign lesions. Fully training the CNN on a large set of annotated CRC samples provides good classification accuracy (around 90% in our tests), but on the other hand has the drawback of a very computationally intensive training procedure. Hence, in our work we also investigate the use of transfer learning approaches, based on CNN models pre-trained on a completely different dataset (i.e. the ImageNet). In our results, transfer learning considerably outperforms the CNN fully trained on CRC samples, obtaining an accuracy of about 96% on the same test dataset.

1 INTRODUCTION

Colorectal carcinoma (CRC) is one of the most diffused cancers worldwide and one of the leading causes of cancer-related death. According to recent epidemiological data, this type of cancer has significant burden in most of the European countries, and it is still associated with very high mortality rates (Marley and Nan, 2016). Hence, the early diagnosis and differentiation of the tumour is crucial for the survival and well-being of a large number of patients.

Traditionally, pathologists perform CRC diagnosis by visually examining under the microscope the resected tissue samples, fixed and stained by means of Hematoxylin and Eosin (H&E). The presence and level of malignancy is assessed by observing the organisational changes in the tissues, which are highlighted by the two stains. As shown in Figure 1, normal colon tissues have a well-defined organisation, with the epithelial cells forming glandular structures and the non-epithelial cells (i.e. stroma) lying in between these glands. The main benign precursor of CRC, adenoma, is characterised by enlarged, hyperchromatic and elongated nuclei arranged in a typically stratified configuration. Compared to normal tissues, the adenoma is characterised by either tubular or villous (finger-like) tissue architecture. Adenocarcinomas, on the other hand, produce abnormal glands that infiltrate into the surrounding tissues.

As it is widely pointed out by literature, manual examination has two major drawbacks. First, it is time-consuming, especially for large image datasets.
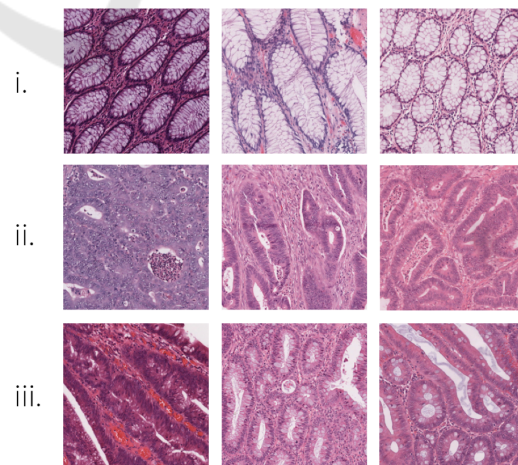

Figure 1: Histological H&E images of colorectal tissues (cropped patches). i) Healthy tissue; ii) Adenocarcinoma; iii) Tubulovillous adenoma.

Second, it is highly subjective and affected by

variability, both inter and intra observer (A. Young and Kerr, 2011). Hence, there are growing efforts towards the development of computer-aided diagnostic techniques, with two major directions: (i) automated segmentation, aimed at partitioning the heterogeneous colorectal samples into homogeneous (i.e. containing only one type of tissue) regions of interest. (ii) automated classification, aimed at categorising the homogeneous tissue regions into a number of classes, either normal or malignant, based upon quantitive features extracted from the image. In both the tasks, the main challenge to be tackled is the extreme intra-class and inter-dataset variability, that is an inherent characteristic of histological imaging. In this work, we focus on the automated classification task, and specifically into three histological categories that are most relevant for CRC diagnosis: (i) healthy tissue, (ii) adenocarcinoma, (iii) tubulovillous adenoma.

In the last few years, the literature on automated classification of histological images has been extensive, with applications covering different anatomical parts other than colon, such as brain, breast, prostate and lungs. Most of the proposed approaches rely on automated texture analysis, where a limited set of local descriptors are computed from patches of the original input images and then fed into a classifier. Among the most frequently used, statistical features based on grey level co-occurrence matrix (GLCM), local binary patterns (LBP), Gabor and wavelet transforms, etc. The texture descriptors, eventually encoded into a compact dictionary of visual words, are used as input of machine learning techniques such as Support Vector Machines (SVM), Random Forests or Logistic Regression classifiers (Di Cataldo and Ficarra, 2017). In spite of the good level of accuracy obtained by some of these works, the dependence on a fixed set of handcrafted features is a major limitation to the robustness of the classical texture analysis approaches. First, because it requires a deep knowledge of the image characteristics that are best suited for classification, which is not obvious. Second, because it puts severe constraints to the generalisation and transfer capabilities of the proposed classifiers, especially in presence of inter-dataset variability.

As an answer to such limitations, in the recent years the use of deep learning (DL) architectures, and more specifically Convolutional Neural Networks (CNNs), has become a major trend (Janowczyk and Madabhushi, 2016; Korbar et al., 2017). In CNNs a number of convolutional and pooling layers learns by backpropagation a set of features that are best for classification, thus avoiding the extraction of handcrafted texture descriptors. Nonetheless, the necessity of training the networks with a huge number of in-

dependent histological samples is still an open issue, which limits the usability of the approach in the everyday clinical setting. Transfer learning (i.e applying CNNs pre-trained on a different type of images, for which large datasets are available) seems a promising solution to this problem (Weiss et al., 2016) but not fully investigated for CRC classification.

In this work. we evaluate a CNN-based approach to automatically differentiate healthy tissues and tubulovillous adenomas from cancerous samples, which is a challenging task in histological image analysis. For this purpose, we fully train a CNN on a large set of colorectal samples, and assess its accuracy on an independent test set. This technique is experimentally compared with two different transfer learning approaches, both leveraging upon a CNN pre-trained on a completely different image dataset. The first approach uses the pre-trained CNN to extract a set of discriminative features that will be fed into a separate Support Vector Machines classifier. The second approach fine-tunes on CRC histological images only the last stages of the pre-trained CNN. By doing so, we investigate and discuss the transfer learning capabilities of CNNs in the domain of colorectal tissues classification.

2 MATERIALS AND METHODS

2.1 Colorectal Cancer Image Dataset

The dataset used in this study was extracted from a public repository of H&E stained whole-slide images (WSIs) of colorectal tissues, available on line at http://www.virtualpathology.leeds.ac.uk/. All the slides are freely available for research purposes, together with their anonymised clinical information.

In order to obtain a statistically significant dataset in terms of inter-subjects and inter-class variability, 27 WSIs were selected among univocal subjects (i.e. one WSI per patient). Note that different types of tissues (e.g. healthy and cancerous portions) coexist in a single WSI. With the supervision of a skilled pathologist, we identified large regions of interest (ROIs) on the WSIs as in the example of Figure 3, so that each ROI is univocally associated to one out of the three tissue subtypes: (i) adenocarcinoma (AC); (ii) tubuvillous adenoma (TV) and (iii) healthy tissue (H). Then, the ROIs were cropped into a total number of 13500 1089x1089 patches (500 per patient), at a magnification level of 40x.

For training and testing purposes, the original image cohort was randomly split into two disjoint subsets, comprising 18 subjects for training (9000
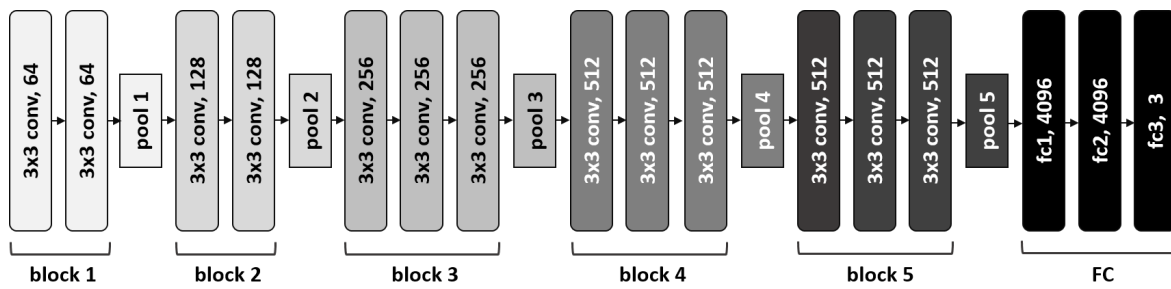
Figure 2: CNN architecture.

patches in total) and 9 for testing (4500 patches). See Table 1 for a complete characterisation of the two sets. The random sampling was stratified, so that both the training and the testing dataset are balanced among the three classes of interest (H, AC and TV, respectively).

Table 1: CRC image dataset.

	Train	Test	Tot
# of patients	18	9	27
# of ROIs	85	24	109
# of patches	9000	4500	13500

Before being fed into the CNN, each patch was down sampled by a factor five, which was empirically set as a trade-off between computational burden of the processing and architectural detail of the images. In order to compensate for the color inconsistencies, the patches were normalised by mean and standard deviation, computed over the whole training dataset.

2.2 Convolutional Neural Network: Architecture and Training Paradigm

A Convolutional Neural Network (CNN) is made up of multiple locally connected trainable stages, piled one after the other, with two or more fully-connected layers as the last step. The first part of the network
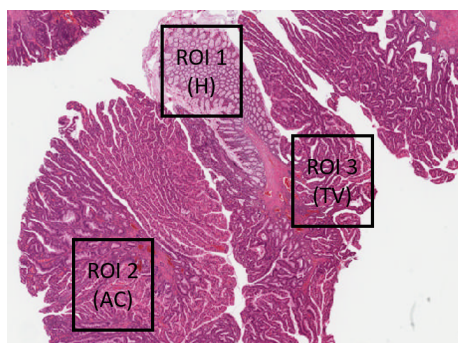

Figure 3: Identification of ROIs from a WSI: example.

is devoted to learning the image representation, with successive layers learning features at a progressively increasing level of abstraction, while the last fully-connected part is devoted to classification and acts like a traditional multilayer perceptron.

From a computational point of view, a CNN architecture is characterised by two main types of building blocks:

(i) **Convolutional (CONV)** blocks, that perform a 2D convolution operation (i.e. kernel filtering) on the input image and apply a non-linear transfer function, such as Rectified Linear Unit (ReLU). Based on the trainable parameters of the kernels, the stage detects different types of local patterns on the input image.

(ii) **Pooling (POOL)** blocks, that perform a non-linear down-sampling of the input (e.g. by applying a max function). This has the double effect of reducing the amount of parameters of the network to control overfitting and of making the image representation (i.e. the local pattern descriptors learnt by the network) spatially invariant.

The number of CONV and POOL blocks (i.e. the depth) of the network is directly related to the level of detail that can be achieved in the the hierarchical representation of the image. Nonetheless, a higher depth also translates into a higher number of parameters, and hence on a higher computational cost.

The training paradigm chosen for the CNN is a classic backpropagation scheme: an iterative process that involves multiple passes of the whole input dataset until the model converges. At each training step, the whole dataset flows from the first to the last layer in order to compute a classification error, quantified by a loss function. Such error flows backward through the net, and at each training step the model parameters (i.e. the network weights) are tuned in the direction that minimises the classification error on the training data.

As a trade-off between representation capabili-

ties and computational costs, in our work we used a VGG16 CNN model, which is represented in Figure 2 (Simonyan and Zisserman, 2014). This architecture was successfully applied to a large number of computer vision tasks. In spite of the quite large depth, the VGG16 adopts a very simple architecture, based on piling up only 3x3 convolution and 2x2 pooling blocks. More specifically, the model consists of 13 CONV layers that can be conceptually grouped into 5 macro-blocks ending with one POOL layer each, and of a final 3-layered fully-connected (FC) stage. Non-linearities are all based on ReLU, except for the last fully-connected layer (FC3), that has a softmax activation function. The convolution stride and the padding are fixed to 1 pixel and the max pooling stride to 2. Differently from the original architecture of VGG16, in our work the size of FC3 is 3, matching the number of categories targeted by our research problem.

The net was built within Keras framework (Chollet et al., 2015) and trained with a backpropagation paradigm. More specifically, we applied a stochastic gradient descent (SGD), implemented with a momentum update approach (Qian, 1999) as iterative optimisation algorithm to minimise the categorical cross-entropy function between the three classes of interest (H, AC and TV). To monitor the training and optimise the choice of hyper-parameters of the net, we used 10% of the training set as validation data. This subset is completely independent from the images used for testing purposes, and was solely used to compute the validation accuracy metric upon which the training process is optimised. Based on validation, we selected a learning rate (LR) of 0.0001, a momentum (M) of 0.9 and a batch size (BS) of 32 images. The learning strategy involved the so-called *early stopping* (i.e., the training is stopped when validation accuracy does not improve for 10 subsequent epochs), as well as the progressive reduction of LR each time the validation accuracy does not improve for 5 consecutive epochs. Such technique was found to largely reduce overfitting (Yao et al., 2007).

The CNN was trained for 30 epochs on our colorectal cancer training dataset, which lasted 8 hours on Linux Infiniband-QDR MIMD Distributed Shared-Memory Cluster provided with single GPU (NVIDIA Tesla K40 - 12 GB - 2880 CUDA cores). Figure 4 shows the loss (a) and accuracy (b) curves on both the training and validation datasets.

From the graphs of Figure 4 we can derive the following observations:

 (i) The model seems to converge quite quickly. Indeed, while training accuracy is still increasing, the value of validation accuracy saturates within

15 epochs.

 (ii) The decay speed of the validation loss curve indicates that the learning rate is appropriate.

(iii) The similarity of validation and training accuracies reasonably rules out overfitting.

2.3 Transfer Learning From Pre-trained CNN

A CNN is a cascade of trainable filter banks, where the first blocks of filters are devoted to the detection of low-level features (i.e. edges or simple shapes), and the following ones are activated by high-level semantic aggregations of the previous patterns. While the top-most blocks are generally tailored to a specific classification task, the lower-level features are ideally generalisable to a large number of applications. This concept, that is at the basis of all the transfer learning techniques using CNNs as feature generators, leverage on the assumption that the network had first been trained on a very large set of examples, with significant variability of image characteristics.

In our work, we performed experiments using a pre-trained CNN model with the same architecture and building blocks of the one used for full training on colorectal cancer images (VGG16, shown in Figure 2). The model was pre-trained on the ImageNet dataset, from the Large Scale Visual Recognition Challenge 2012 (ILSVRC-2012). The Ima-
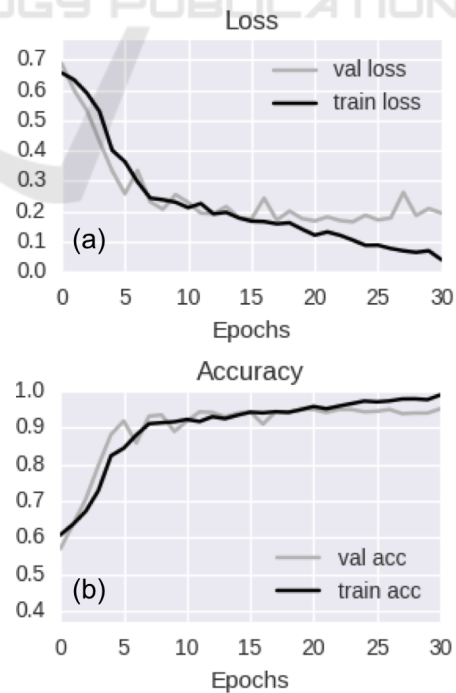

Figure 4: Training vs validation loss per epoch (a) and training vs validation accuracy per epoch (b).
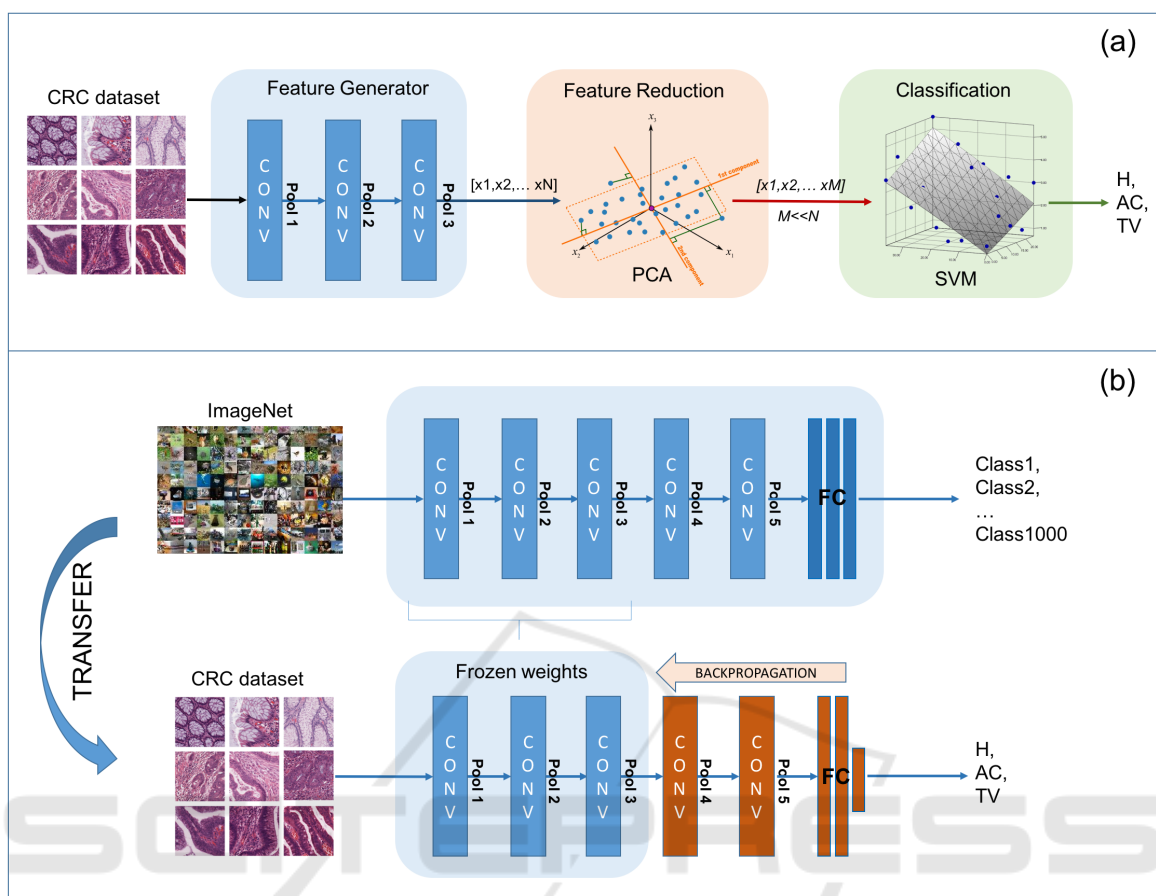
Figure 5: Transfer learning approaches. (a) Pre-trained CNN as a fixed feature generator. (b) Fine tuning of pre-trained CNN.

geNet dataset contains 1.2 million photographs depicting 1000 different categories of natural objects. Hence, the content and characteristics of the training images are completely different from our specific target.

To apply the pre-trained CNN to our histology classification task, we implemented and compared two different transfer learning approaches, whose main steps are represented in Figure 5 (a) and (b), respectively:

(i) **CNN as a fixed feature generator.** The histological images are given as input to the pre-trained CNN for inference. The features extracted by the convolutional blocks are then fed into a separate machine learning framework, consisting of a feature reduction stage and a supervised classifier.

(ii) **Fine-tuning the CNN.** The CNN model is re-trained on our training set of histological images, keeping all the parameters of the low-level blocks fixed to their initial value. Hence, only the weights of the top-most layers are fine-tuned

for colorectal cancer classification.

As a preliminary step to both the two approaches, we analysed the discriminative capabilities of the features generated by all the major blocks of the pre-trained CNN. More specifically, we randomly selected a small subset of the training images (i.e. 1500 patches, 500 per class) and we fed these images into the pre-trained CNN. The output of each successive macro-block of the CNN was then analysed, to assess the degree of separation of samples belonging to the three different classes. As a trade-off between thoroughness and computational burden of the investigation, we analysed the intermediate output of the CNN only at the end of the pooling layers (i.e. POOL1 to 5, in Figure 2). Indeed, as the pooling layers perform a feature reduction on the output of the convolutional filters, they are expected to produce a non-redundant set of image features compared to CONV layers.

The degree of class separation was assessed by means of t-Distributed Stochastic Neighbour Embedding (t-SNE) (Maaten and Hinton, 2008), a non-linear dimensionality reduction algorithm that is used for

the visualisation of high-dimensional datasets in a reduced 3-dimensional space. More specifically, t-SNE models each high-dimensional object (in our case, the feature vector obtained at the output of a POOL layer) by means of or three-dimensional point in a cartesian space, so that similar feature vectors are represented by nearby points and dissimilar vectors by distant points. This allows to qualitatively assess the class separability in the original feature space, and hence to establish the POOL block that ensures the best class separability (see examples in Figure 6).

The outcome of t-SNE was confirmed by further quantitative experiments, based on assessing the classification performance of a separate classifier trained on different POOL blocks. In all such experiments, POOL3 outperformed all the other blocks.

2.3.1 Pre-trained CNN as A Fixed Feature Generator

As first transfer learning methodology, the output of the most discriminative POOL layer of the pre-trained CNN (in our case POOL3) was used to generate a feature vector for colorectal cancer classification. The feature vector was fed into the machine learning framework represented by Figure 5-(a), consisting in a feature reduction and a classification step.

(i) **Feature reduction.** Principal Component Analysis (PCA) was applied to reduce the dimensionality of the input data and prevent overfitting. PCA performs an orthogonal transformation of the original features into the so-called principal components, a new group of values which are linear combinations of the original characteristics. As PCA works towards the minimisation of the correlation between the features, the new data representation is expected to best summarise those features which are most representative for the classes of interest. In our work, the optimal number of principal components was empirically determined by means of a sequential forward procedure. The mean clas-
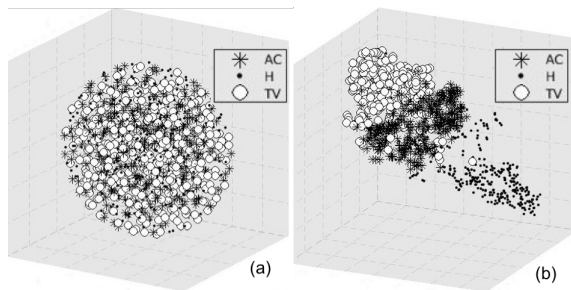
sification accuracy obtained on the training set was computed at increasing number of principal components, with a step of 50. To limit the computational cost of the procedure, we selected the minimum number of principal components after which the classification accuracy had started decreasing, that was equal to 250 (see Figure 7).

(ii) **Classification.** The final classification into three categories (H, AC, TV) was performed by a Support Vector Machine (SVM) with a Gaussian radial basis function kernel. The hyperparameters of the kernel were set by means of a Bayesian Optimisation (BO) algorithm (Hastie et al., 2009), implementing a 10-fold cross-validation procedure on the training images. BO was found to provide much better and faster results compared to classic methods based on grid search or heuristic techniques.

2.3.2 Fine-tuning of Pre-trained CNN

As a second transfer learning methodology, we tried to adapt the pre-trained VGG16 net to our specific classification task. For this purpose, we first initialised all the weights of the network to the ones determined on the ImageNet dataset, as represented in Figure 5-(b). Then, we continued the backpropagation procedure on our CRC dataset, keeping the weights of the first blocks of the net frozen. More specifically, we froze all the weights up-to the most discriminative pooling layer (POOL3), as determined by t-SNE in Section 2.3. The rationale of such strategy is trying to maintain the low-level features describing the most generic and generalisable details

Figure 6: t-SNE visualisation of the output of POOL2 (a) and POOL3 (b).
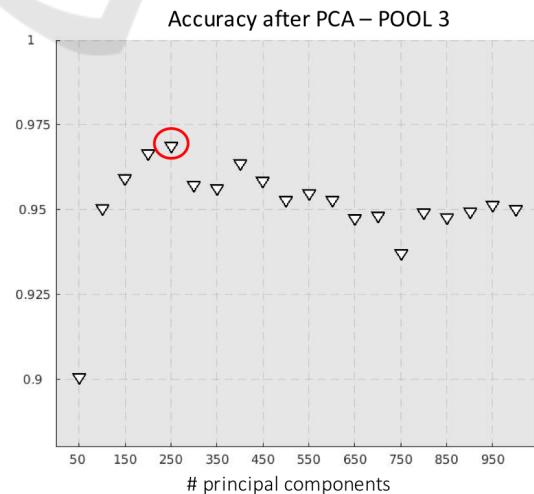

Figure 7: Sequential forward procedure to select the optimal number of principal components for PCA.

(e.g. edges and simple shapes) as they were learnt from the ImageNet. Hence, all the computational power can be devoted to the training of the top-most layers, which are expected to learn high-level task-specific features for colorectal image classification. The training strategy was exactly the same that was described in Section 2.2.

3 CLASSIFICATION ACCURACY

3.1 Performance Metrics

The classification performance was assessed using the dataset described in Section 2.1. As already pointed out, the test dataset is completely independent from the one used for training the network and optimising the classification parameters. The accuracy of the system was assessed at two different levels of abstraction (per patch and per patient, respectively). For this purpose, we introduce two different performance metrics.

(i) **Patch score:** (S_P), defined as the fraction of patches of the test set that were correctly classified:

$$S_P = \frac{N_C}{N},$$

where N_C is the number of correctly classified patches and N the total number of patches in the test set.

(ii) **Patient score:** (S_{Pt}), defined as the fraction of patches of a single patient that were correctly classified (i.e. *per-patient* patch score), averaged over all the patients in the test set:

$$S_{Pt} = \frac{\sum_i S_P(i)}{N_P},$$

where $S_P(i)$ is the patch score of the $i-th$ patient and N_P the total number of patients in the test set.

3.2 Results and Discussion

In Table 2 we report both the patch and patient scores obtained for the three classification frameworks described in Section 2. More specifically:

(i) **full-train-CNN** refers to the CNN fully trained on CRC samples.

(ii) **CNN+SVM:** refers to the SVM, with pre-trained CNN used as fixed feature generator.

(iii) **fine-tune-CNN:** refers to the pre-trained CNN with fine-tuning of the final stages.

For the patient score, S_{Pt} value is reported as mean $\pm$ standard deviation. From the results of Table 2 we can observe that all the proposed classification frameworks obtained accuracy (both patch and patient-wise) above 90%. Hence, the promising results obtained by CNNs in other contexts are confirmed even for the application targeted by our work. On top of that, the accuracy computed over all the patches of the test set (S_P) is very similar to the one computed patient per patient (S_{Pt}), with a very small standard deviation of the latter value. This suggests that the classification frameworks are all quite robust and cope well with inter-patient variability, that is a typical challenge of histopathological image analysis.

The same conclusions hold if we analyse the per-class results, that are reported in the form of 3X3 confusion matrices in Figure 8. In addition, from the confusion matrices we can observe that the performance of the classification frameworks is fairly homogeneous for the three classes H, AC and TV.

Quite interestingly, both the methodologies based on transfer learning overcome the accuracy obtained by the CNN fully trained on colorectal samples by almost 7%. In particular, the approach that provided the best accuracy values (both patch and patient-wise) was the pre-trained CNN with fine-tuning of the blocks following POOL 3. This suggests the following:

(i) Even though the full training seemed to converge well and without overfitting on the training images (see Figure 4), the CNN would probably necessitate a much larger cohort of examples to learn features that are sufficiently general to cope with the high variability of histopathological images. On the other hand, much larger training datasets would make the learning process prohibitive, especially in a clinical context.

(ii) In spite of the fact that the pre-training was performed on a completely different dataset (i.e. the ImageNet, which contains photographs of every-day objects and natural scenes, and not histological samples), the low-level features learnt by the first stages of a CNN can be successfully generalised to the context of CRC image classification. Hence, CNNs are as a matter of fact capable of extracting usable semantic knowledge from totally different domains. This is very encouraging, as it partially avoids

Table 2: Patch and patient scores on the test set.

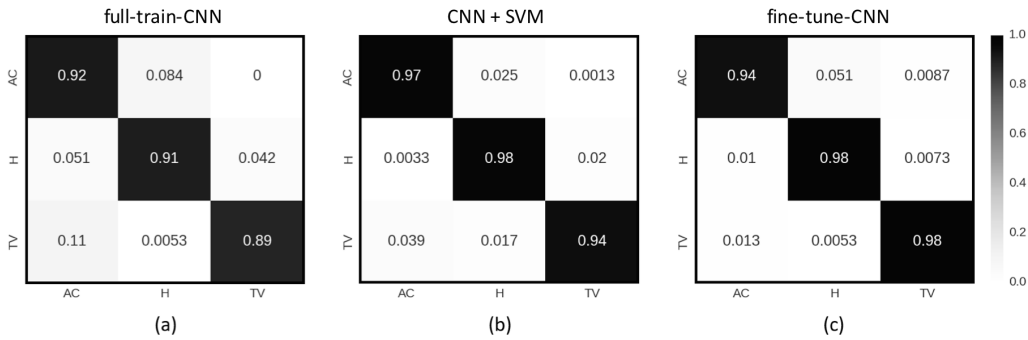|	S_P	S_{Pt}
full-train-CNN	0.9037	0.9022 ($\pm$ 0.0155)
CNN+SVM:	0.9646	0.9667 ($\pm$ 0.0082)
fine-tune-CNN	0.9682	0.9678 ($\pm$ 0.00092)

Figure 8: Patch-wise confusion matrices for (a) CNN fully trained on CRC samples, (b) SVM with pre-trained CNN as fixed features generator, (c) pre-trained CNN with fine-tuning of the stages after POOL3 block.

the computational problems and overfitting risks associated with full-training. Indeed, the fine-tuning of the pre-trained CNN took only two hours against the eight taken by full-training, using the same hardware and learning paradigm.

To investigate further on the performance of the fine-tuned CNN, we run additional experiments by changing the starting block for the backpropagation algorithm. In Figure 9, we report the patch score obtained on the test set, for different configurations of the fine-tuning. In the *x*-axis, *POOL-i* means that only the weights after the *i*-th POOL block were learnt on the CRC training set, while all the rest of the parameters were frozen to the values learnt on the ImageNet. Likewise, *FC* means that only the fully-connected stage of the network was trained. The trend of the patch score values shows that the maximum accuracy is reached when the CNN is fine-tuned after POOL3, which confirms the qualitative results of t-SNE. On top of that, we can observe that fully-training the network obtains more or less the same results than training only the last fully-connected stage. This further confirms that CNN can be successfully used to transfer features learnt from the ImageNet.

4 CONCLUSIONS AND FUTURE WORK

In this work we investigated the use of deep learning, and more specifically of Convolutional Neural Networks, for the automated classification of colorectal histology samples into three main classes of interest: healthy tissue, adenocarcinoma or tubulovillous adenoma.

For this purpose, we applied a CNN with VGG16 architecture, which we fully trained on a large dataset of pre-annotated images of colorectal samples. This solution provided satisfactory results when applied to

an independent test dataset, with classification accuracy in the order of 90%.

Besides the traditional full training approach, we investigated two types of transfer learning techniques: (i) using the first convolutional stages of a CNN pre-trained on the ImageNet as a fixed feature generator for a Support Vector Machine, with a preliminary feature reduction step; (ii) using the colorectal training set to fine-tune the last convolutional and fully-connected stages of the pre-trained CNN.

In our experiments the transfer learning techniques outperform the full training approach both in terms of classification accuracy (above 96%) as well as in terms of training time. Hence, they demonstrate that low-level features learnt by the CNN in a very different context (the ImageNet, in this case) can be successfully transferred to the classification of colorectal images.

As a future work, we plan to extend the classification problem to more tissue categories (i.e. different types of benign lesions, besides tubulovillous adenoma). In the long run, we plan to design a develop a complete framework for the analysis of colorectal WSIs based on CNNs.
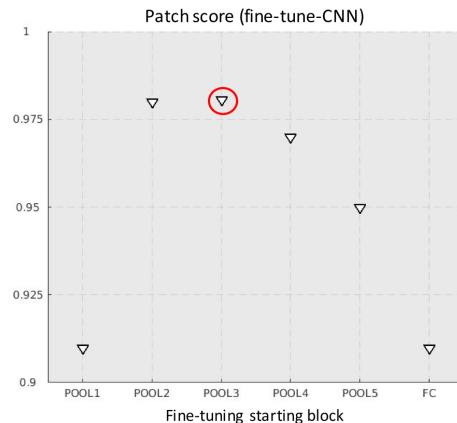

Figure 9: Mean accuracy in relation to the first block till back-propagation is continued.

REFERENCES

A. Young, R. H. and Kerr, D. (2011). *ABC of Colorectal Cancer*. Wiley-Blackwell, 2nd edition.

Chollet, F. et al. (2015). Keras. https://github.com/fchollet/keras.

Di Cataldo, S. and Ficarra, E. (2017). Mining textural knowledge in biological images: Applications, methods and trends. *Computational and Structural Biotechnology Journal*, 15:56 – 67.

Hastie, T., Tibshirani, R., and Friedman, J. (2009). Overview of supervised learning. In *The elements of statistical learning*. Springer.

Janowczyk, A. and Madabhushi, A. (2016). Deep learning for digital pathology image analysis: A comprehensive tutorial with selected use cases. *Journal of Pathology Informatics*, 7(1):29.

Korbar, B., Olofson, A. M., Miraflor, A. P., Nicka, C. M., Suriawinata, M. A., Torresani, L., Suriawinata, A. A., and Hassanpour, S. (2017). Deep learning for classification of colorectal polyps on whole-slide images. *Journal of Pathology Informatics*, 8:30.

Maaten, L. v. d. and Hinton, G. (2008). Visualizing data using t-sne. *Journal of Machine Learning Research*, 9(Nov):2579–2605.

Marley, A. R. and Nan, H. (2016). Epidemiology of colorectal cancer. *International Journal of Molecular Epidemiology and Genetics*, 7(3):105–114.

Qian, N. (1999). On the momentum term in gradient descent learning algorithms. *Neural networks*, 12(1):145–151.

Simonyan, K. and Zisserman, A. (2014). Very deep convolutional networks for large-scale image recognition. *arXiv preprint arXiv:1409.1556*.

Weiss, K., Khoshgoftaar, T. M., and Wang, D. (2016). A survey of transfer learning. *Journal of Big Data*, 3(1):9.

Yao, Y., Rosasco, L., and Caponnetto, A. (2007). On early stopping in gradient descent learning. *Constructive Approximation*, 26(2):289–315.